

Graphical Synopsis

Special Issue: Dedicated to Professor Dr. Ulrich Müller on the occasion of his 80th birthday

Laudatio/Preface

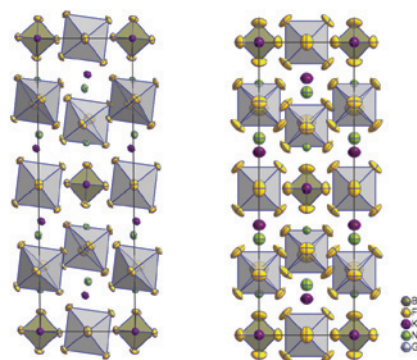
Jascha Bandemehr, Josefin Klippstein,
Sergei I. Ivlev, Malte Sachs and Florian
Kraus

Laboratory synthesis and characterization of Knasibfite

**$K_3Na_4[SiF_6]_3[BF_4]$ and the homologous Ge
compound $K_3Na_4[GeF_6]_3[BF_4]$**

<https://doi.org/10.1515/zkri-2019-0068>
Z. Kristallogr. 2020; 235(8–9): 247–254

Synopsis: Knasibfite occurs in nature as the only mineral containing $[BF_4]^-$ and $[SiF_6]^{2-}$ anions. We present a laboratory synthesis, the crystal structure, and its IR and Raman spectra. The homologous compound $K_3Na_4[GeF_6]_3[BF_4]$ is reported as well. Phase transition temperatures of the compounds were determined by heat capacity measurements. The crystal structures of the monoclinic low-temperature (space group $I121$) and the orthorhombic higher-temperature polymorphs (space group $Im2m$) are related by a *translationengleiche* step of index 2.

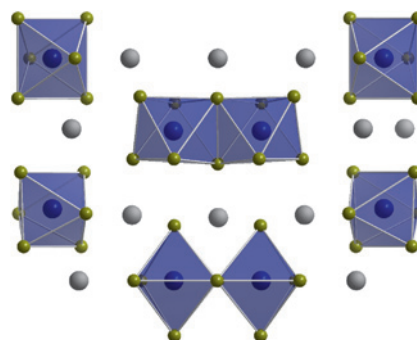


Jen-Hui Chang, Thomas Doert and Michael
Ruck

The crystal structures of α -Rb₇Sb₃Br₁₆, α - and β -Tl₇Bi₃Br₁₆ and their relationship to close packings of spheres

<https://doi.org/10.1515/zkri-2020-0013>
Z. Kristallogr. 2020; 235(8–9): 255–261

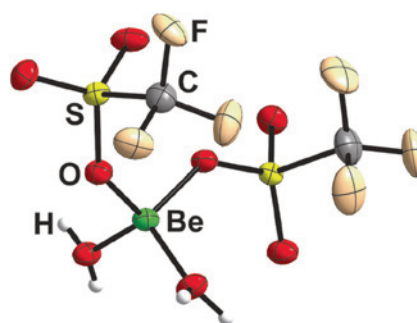
Synopsis: α -Tl₇Bi₃Br₁₆ and α -Rb₇Sb₃Br₁₆ (both adopting the Tl₇Bi₃I₁₆ structure type) and β -Tl₇Bi₃Br₁₆ (new structure type) comprise slabs of isolated $[EX_6]^{3-}$ -octahedra and $[E_2X_{10}]^{4-}$ -octahedra pairs, which can topologically be described as sphere close packing.



Matthias Müller and Magnus R. Buchner
**Beryllium triflates: synthesis and
structure of $BeL_2(OTf)_2$ ($L=H_2O$, THF,
 nBu_2O)**

<https://doi.org/10.1515/zkri-2020-0016>
Z. Kristallogr. 2020; 235(8–9): 263–268

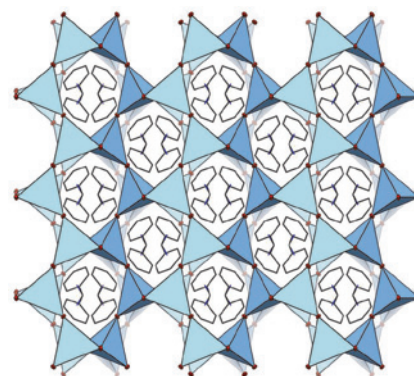
Synopsis: The beryllium triflates $Be(H_2O)_2(OTf)_2$, $Be(OTf)_2(THF)_2$ and $Be(nBu_2O)_2(OTf)_2$ were synthesized and characterized via single crystal X-ray diffraction. The observed Be–O atomic distances between Be^{2+} and the triflate anions in solid state are the shortest known distances of this kind found in a metal triflate yet.



Natalie Dehnhardt, Chantsalmaa Berthold, Kevin Dollberg, Frank Tambornino and Johanna Heine
Synthesis and crystal structures of two layered Cu(I) and Ag(I) iodidometalates

<https://doi.org/10.1515/zkri-2020-0021>
 Z. Kristallogr. 2020; 235(8–9): 269–273

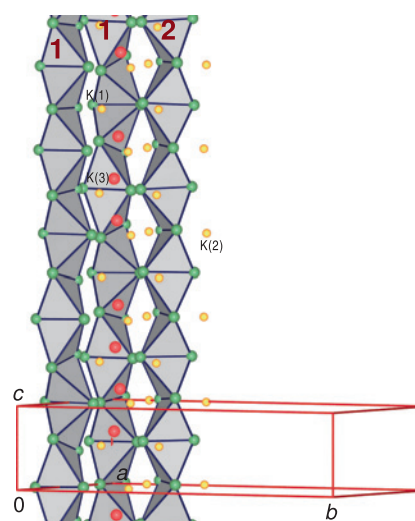
Synopsis: Two new layered Cu(I) and Ag(I) iodidometalates have been prepared using benzylammonium as a counterion.



Michael Schwarz, Pirmin Stüble, Katharina Köhler and Caroline Röhr
New mixed-valent alkali chain sulfido ferrates $A_{1+x}[FeS_2]$ ($A = K, Rb, Cs$; $x = 0.333–0.787$)

<https://doi.org/10.1515/zkri-2020-0023>
 Z. Kristallogr. 2020; 235(8–9): 275–290

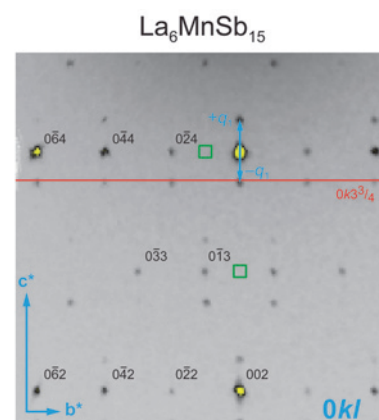
Synopsis: Undulated tetrahedra chains in the (3+1)D modulated crystal structure of the mixed-valent sulfido ferrate salt $K_{7.15}[FeS_2]_4$.



Mathis Radzieowski, Steffen Klenner, Rolf-Dieter Hoffmann and Oliver Janka
Structure solution of incommensurately modulated La_6MnSb_{15}

<https://doi.org/10.1515/zkri-2020-0034>
 Z. Kristallogr. 2020; 235(8–9): 291–301

Synopsis: La_6MnSb_{15} was synthesized from elements in quartz ampoules, the crystal structure was investigated via single-crystal X-ray diffraction experiments leading to the observation of superstructure reflections. The structure could be solved and refined in superspace group $Immm(00\gamma)000$. Additionally, the temperature dependence of the electrical resistivity was investigated and ^{121}Sb Mößbauer-spectroscopic measurements at 78 K were conducted.

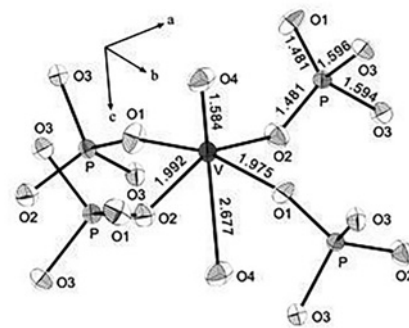


Sven Umlauf, Markus Weber and Robert Glaum

Polymorphs of $\text{VO}(\text{PO}_3)_2$: synthesis and crystal structure refinement revisited

<https://doi.org/10.1515/zkri-2020-0037>
Z. Kristallogr. 2020; 235(8–9): 303–309

Synopsis: Single crystals of β - $(\text{V}^{\text{IV}}\text{O})(\text{PO}_3)_2$ were grown in a sealed silica ampoule with chlorine as mineralizer. The crystal structure of the orthorhombic (pseudo-tetragonal) β -polymorph was refined from X-ray single-crystal data [pseudomerohedral twin, $Fdd2$, $Z = 8$, $a = 15.536(2) \text{ \AA}$, $b = 15.586(2) \text{ \AA}$, $c = 4.2611(5) \text{ \AA}$, $R_1 = 0.0322$, $wR_2 = 0.068$ for 1072 unique reflections with $F_o > 4\text{sig}(F_o)$, 50 variables]. Earlier reports on a tetragonal polymorph with unusual geometric structure of the $[(\text{V}=\text{O})\text{O}_5]$ polyhedron are corrected.

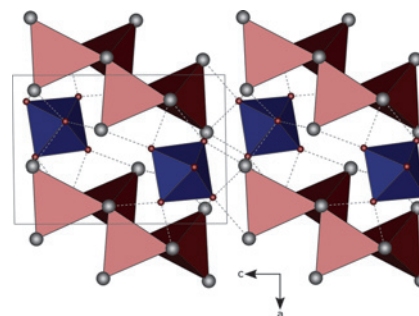


Stephan G. Jantz, Florian Pielhofer and Henning A. Höppe

On tungstates of divalent cations (III) – $\text{Pb}_5\text{O}_2[\text{WO}_6]$

<https://doi.org/10.1515/zkri-2020-0041>
Z. Kristallogr. 2020; 235(8–9): 311–317

Synopsis: The new lead tungstate $\text{Pb}_5\text{O}_2[\text{WO}_6]$ comprises $[\text{Pb}_{10}\text{O}_4]^{12+}$ oligomers and non-condensed WO_6 octahedra and is obtained as yellowish powder in accordance with a band-gap of 2.8 eV (calculated by DFT: 2.9 eV).

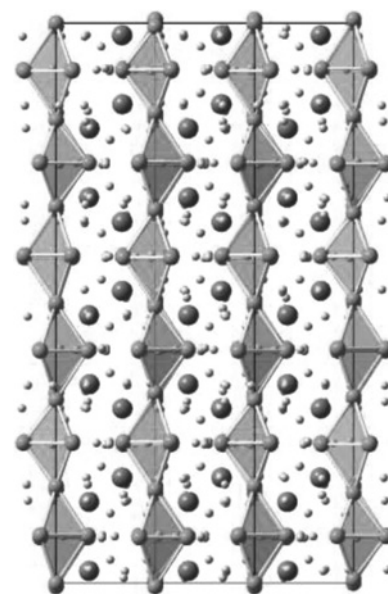


Holger Kohlmann

Hydrogen order in Laves phases hydrides

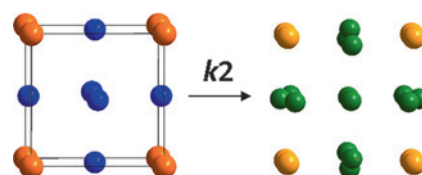
<https://doi.org/10.1515/zkri-2020-0043>
Z. Kristallogr. 2020; 235(8–9): 319–332

Synopsis: Order-disorder phase transitions in Laves phase hydrides are described concisely using *Bärnighausen* trees.



Julia-Maria Hübner, Wilder Carrillo-Cabrera, Raul Cardoso-Gil, Primož Koželj, Ulrich Burkhardt, Martin Etter, Lev Akselrud, Yuri Grin and Ulrich Schwarz
High-pressure synthesis of SmGe_3

Synopsis: The high-pressure phase SmGe_3 adopts a new $2 \times 2 \times 2$ superstructure of the Cu_3Au motif, thus representing a distorted binary variant of *fcc*.

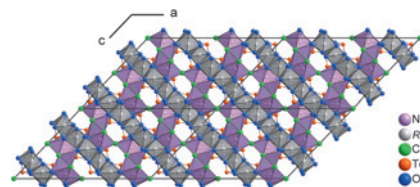


<https://doi.org/10.1515/zkri-2020-0058>
 Z. Kristallogr. 2020; 235(8–9): 333–339

Stefan Greiner, Sabine Zitzer, Sabine Strobel, Peter S. Berdonosov and Thomas Schleid

The complete series of sodium rare-earth metal(III) chloride oxotellurates(IV) $\text{Na}_2\text{RE}_3\text{Cl}_3[\text{TeO}_3]_4$ ($\text{RE} = \text{Y, La–Nd, Sm–Lu}$)

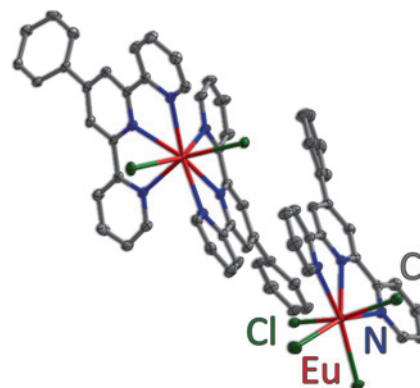
Synopsis: The oxotellurates $\text{Na}_2\text{RE}_3\text{Cl}_3[\text{TeO}_3]_4$ crystallize in the monoclinic space group no. 15, but their structure was described in different settings (*C2/c* and *A2/n*) with almost the same metrics. Now the complete series ($\text{RE} = \text{Y, La–Nd, Sm–Lu}$) is uniformly available with the *Pearson* symbol *mC96* and the *Wyckoff* sequence $f^{11}ea$.



<https://doi.org/10.1515/zkri-2020-0051>
 Z. Kristallogr. 2020; 235(8–9): 341–352

Alexander E. Sedykh, Robin Bissert, Dirk G. Kurth and Klaus Müller-Buschbaum
Structural diversity of salts of terpyridine derivatives with europium(III) located in both, cation and anion, in comparison to molecular complexes

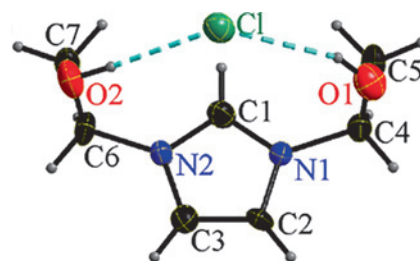
Synopsis: Variation of the backside of terpyridyl-ligands gives salt-like Eu-compounds with the Ln-cation present in both, cation and anion, whereas additional dipyrindyl ligands function as a linker that result in the crystallization of dimeric complexes.



<https://doi.org/10.1515/zkri-2020-0053>
 Z. Kristallogr. 2020; 235(8–9): 353–363

Kai Richter, Katharina V. Dorn, Volodymyr Smetana and Anja-Verena Mudring
Elucidating structure–property relationships in imidazolium-based halide ionic liquids: crystal structures and thermal behavior

Synopsis: Endowing ionic liquid forming ions with an enhanced hydrogen bonding capacity leads to hydrogen bond frustration and is an additional, effective design tool to suppress the melting point of salts

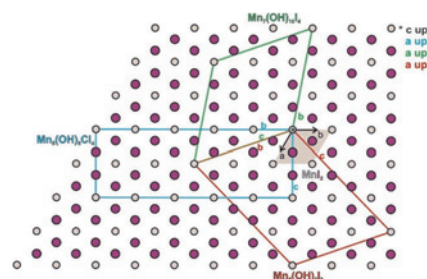


<https://doi.org/10.1515/zkri-2020-0046>
 Z. Kristallogr. 2020; 235(8–9): 365–374

Viktoria Falkowski, Alexander Zeugner, Stefan Seidel, Rainer Pöttgen, Klaus Wurst, Michael Ruck and Hubert Huppertz
Syntheses and crystal structures of the manganese hydroxide halides $\text{Mn}_5(\text{OH})_6\text{Cl}_4$, $\text{Mn}_5(\text{OH})_7\text{I}_3$, and $\text{Mn}_7(\text{OH})_{10}\text{I}_4$

<https://doi.org/10.1515/zkri-2020-0040>
 Z. Kristallogr. 2020; 235(8–9): 375–389

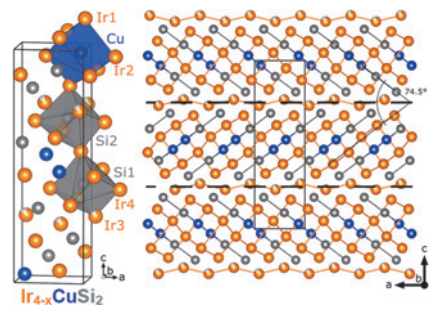
Synopsis: Syntheses and crystal chemical relationships of the new manganese hydroxide halides $\text{Mn}_5(\text{OH})_6\text{Cl}_4$, $\text{Mn}_5(\text{OH})_7\text{I}_3$, and $\text{Mn}_7(\text{OH})_{10}\text{I}_4$ with respect to the aristotype $\text{Mg}(\text{OH})_2$ (brucite).



Jan P. Scheifers and Boniface P. T. Fokwa
Site-preferential copper substitution for silicon leads to Cu-chains in the new ternary silicide $\text{Ir}_{4-x}\text{CuSi}_2$

<https://doi.org/10.1515/zkri-2020-0061>
 Z. Kristallogr. 2020; 235(8–9): 391–399

Synopsis: $\text{Ir}_{4-x}\text{CuSi}_2$, the first ternary silicide in the Ru_4Si_3 -type structure is discovered. Its structure contains Ir vacancies along the twin boundary (see Figure) and exhibits a distorted structure compared to Ru_4Si_3 , as the larger Cu selectively replaces Si on one of three possible sites, leading to zigzag chains with short Cu–Cu distances.



Constantin Hoch
Syntheses and crystal structures of solvate complexes of alkaline earth and lanthanoid metal iodides with *N,N*-dimethylformamide

<https://doi.org/10.1515/zkri-2020-0071>
 Z. Kristallogr. 2020; 235(8–9): 401–411

Synopsis: The crystal structures of solvate complexes of earth alkaline and lanthanoid metal iodides with *N,N*-dimethylformamide (DMF) are described on the basis of single-crystal structures. DMF acts as monodentate ligand with very low sterical demands. The DMF complexes $[\text{M}(\text{DMF})_x]\text{I}_y$ can be taken as starting materials for a number of reactions and are much easier to prepare than the binary metal iodides themselves. The plethora of crystal structures can be compared on the basis of the packing topology of the almost spherical cationic complex units.

